Quantum shuttle: physics of a numerical challenge

Andrea Donarini

Institut für Theoretische Physik, Universität Regensburg,
93040 - Regensburg, Germany.

Summary. Shuttle devices are a class of Nanoelectromechanical systems generically described as movable single electron transistors. They exhibit an electromechanical instability from the standard tunnelling regime to the shuttling regime in which the quantum dot oscillates and transfer one electron per cycle. I present a theory for the device in which both the electrical and mechanical degrees of freedom are quantized. The different operating regimes are detected by analyzing current, noise and Wigner function distributions. The calculation of the stationary solution for the Generalized Master Equation which describes the system dynamics is the starting point for the evaluation of these quantities and represents a numerically challenging problem due to the size of the Hilbert space necessary to capture the tunnelling to shuttling transition.

1 The archetypal model

The archetypal shuttle device (SD) consists of a movable quantum dot (QD) suspended between source and drain leads. One can imagine the dot attached to the tip of a cantilever or connected to the leads by some soft ligands or embedded into an elastic matrix. In the model the nanoparticle is confined to an harmonic potential. We give a schematic visualization of the device in figure 1.

Due to its small diameter, the QD has a very small capacitance and thus a charging energy that exceeds the thermal energy k_BT For this reason we assume that only one excess electron can occupy the device (Coulomb blockade) and we describe the electronic state of the oscillating dot as a two-level system (empty/charged). Electrons can tunnel between leads and dot with tunnelling amplitudes which are exponentially dependent on the position of the central island. This is due to the exponentially decreasing/increasing overlapping of the electronic wave functions.

The Hamiltonian of the model reads:

$$H = H_{\rm sys} + H_{\rm leads} + H_{\rm bath} + H_{\rm tun} + H_{\rm int} \tag{1}$$

where

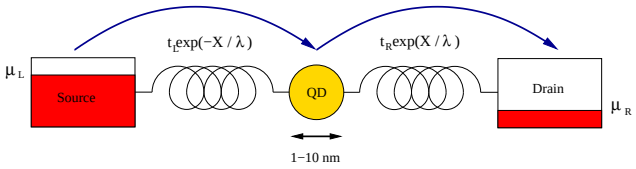

Fig. 1. *Schematic representation of a shuttle device: electrons tunnel from the left lead at chemical potential (μ_L) to the quantum dot and eventually to the right lead at lower chemical potential μ_R. The position dependent tunnelling amplitudes are indicated. X is the displacement from the equilibrium position. The springs represent the harmonic potential in which the central dot can move.*

$$\begin{aligned} H_{\rm sys} &= \frac{\hat{p}^2}{2m} + \frac{1}{2}m\omega^2\hat{x}^2 + (\varepsilon_1 - e\mathcal{E}\hat{x})c_1^\dagger c_1 \\ H_{\rm leads} &= \sum_k (\varepsilon_{l_k} c_{l_k}^\dagger c_{l_k} + \varepsilon_{r_k} c_{r_k}^\dagger c_{r_k}) \\ H_{\rm tun} &= \sum_k [T_l(\hat{x}) c_{l_k}^\dagger c_1 + T_r(\hat{x}) c_{r_k}^\dagger c_1] + h.c. \\ H_{\rm bath} + H_{\rm int} &= \text{generic heat bath} \end{aligned} \tag{2}$$

Using the language of quantum optics we call the movable grain alone *the system*. This is then coupled to two electric baths (the leads) and a generic heat bath. The system is described by a single electronic level of energy ε_1 and a harmonic oscillator of mass m and frequency ω. When the dot is charged the electrostatic force ($e\mathcal{E}$) acts on the grain and gives the *electrical influence* on the mechanical dynamics. The electric field $\mathcal{E}$ is generated by the voltage drop between left and right lead. In our model, though, it is kept as an external parameter, also in view of the fact that we will always assume the potential drop to be much larger than any other energy scale of the system (with the only exception of the charging energy of the dot). The operator form $\hat{x}, \hat{p}$ for the mechanical variables is due to the quantum treatment of the harmonic oscillator. The leads are Fermi seas kept at two different chemical potentials (μ_L and μ_R) by the external applied voltage ($\Delta V = (\mu_L - \mu_R)/e$). The oscillator is immersed into a dissipative environment that we model as a collection of bosons and is coupled to that by a weak bilinear interaction:

$$\begin{aligned} H_{\rm bath} &= \sum_{\mathbf{q}} \hbar\omega_{\mathbf{q}} {d_{\mathbf{q}}}^\dagger d_{\mathbf{q}} \\ H_{\rm int} &= \sum_{\mathbf{q}} \hbar g (d_{\mathbf{q}} + {d_{\mathbf{q}}}^\dagger)(d + d^\dagger) \end{aligned} \tag{3}$$

where the bosons have been labelled by their wave number $\mathbf{q}$. The coupling to the electric baths is introduced by the tunnelling Hamiltonian $H_{\rm tun}$. The tunnelling amplitudes $T_l(\hat{x})$ and $T_r(\hat{x})$ depend exponentially on the position operator $\hat{x}$ and represent the *mechanical feedback* on the electrical dynamics:

$$T_{l,r}(\hat{x}) = t_{l,r} \exp(\mp\hat{x}/\lambda) \tag{4}$$

where λ is the tunnelling length.

2 The Dynamics: Generalized Master Equation

The Hamiltonian for the shuttle device includes terms describing (i) the electronic part of the movable QD, (ii) its mechanical motion (which is quantized), (iii) the position dependent coupling of the QD and the leads, (iv) the leads (treated as non-interacting fermions), and (v) coupling to environment, which damps the mechanical motion [1, 2, 3, 4]. Since we are only interested on the dynamics of the quantum dot, we integrate out the environmental degrees of freedom (the lead electrons, and a generic heat bath) to obtain a Generalized Master Equation for the "system" (= QD + quantized oscillator) density operator:

$$\dot{\sigma}(t) = \mathcal{L}\sigma(t) = (\mathcal{L}_{\rm coh} + \mathcal{L}_{\rm driv} + \mathcal{L}_{\rm damp})\sigma(t). \tag{5}$$

Here $\mathcal{L}_{\rm coh}, \mathcal{L}_{\rm driv}$ and $\mathcal{L}_{\rm damp}$ are superoperators corresponding to the coherent evolution, coupling to leads, and damping of the QD. In the spirit of the classical master equation, it is sufficient to consider the diagonal electronic components (i.e., an empty and an occupied QD, respectively), since the electrical coherences are rapidly damped by the macroscopic leads. Nevertheless a generalization of the original concept that maintain the mechanical coherences is necessary to capture the electromechanical correlation characterizing the shuttle instability. The resulting equation of motion for the reduced density matrix reads:

$$\begin{aligned}
\dot{\sigma}_{00}(t) \;=\; & \frac{1}{i\hbar}[H_{\rm osc}, \sigma_{00}(t)] - \frac{\Gamma_L}{2}(e^{-\frac{2x}{\lambda}}\sigma_{00}(t) \\
& + \sigma_{00}(t)e^{-\frac{2x}{\lambda}}) + \Gamma_R e^{\frac{x}{\lambda}}\sigma_{11}(t)e^{\frac{x}{\lambda}} \\
& + \mathcal{L}_{\rm damp}\,\sigma_{00}(t)\ , \\
\dot{\sigma}_{11}(t) \;=\; & \frac{1}{i\hbar}[H_{\rm osc} - eEx, \sigma_{11}(t)] + \Gamma_L e^{-\frac{x}{\lambda}}\sigma_{00}(t)e^{-\frac{x}{\lambda}} \\
& - \frac{\Gamma_R}{2}(e^{\frac{2x}{\lambda}}\sigma_{11}(t) + \sigma_{11}(t)e^{\frac{2x}{\lambda}}) \\
& + \mathcal{L}_{\rm damp}\,\sigma_{11}(t).
\end{aligned} \tag{6}$$

where

$$\mathcal{L}_{\rm damp}\sigma = -\frac{i\gamma}{2\hbar}[x, \{p, \sigma\}] - \frac{\gamma m\omega}{\hbar}(\bar{N} + 1/2)[x, [x, \sigma]]\ .$$

The physical parameters defining the quantum shuttle are thus the (bare) tunnelling rates between QD and leads $\Gamma_{L/R}$, the oscillator frequency ω, the damping rate of the oscillator γ, the temperature T, and the tunnelling length λ.

3 Stationary state: a mathematical challenge

The master equation generally describes the irreversible dynamics due to the coupling between the system and the infinite number of degrees of freedom of the environment. It is reasonable to require that in absence of a time dependent driving mechanism the system tends asymptotically to a stationary condition defined by the equation:

$$\mathcal{L}\sigma^{\rm stat} = 0 \tag{7}$$

3.1 A matter of matrix sizes

We calculate the stationary matrix σ^{stat} numerically: we have to find the null vector of the matrix representation for the Liouvillean super-operator $\mathcal{L}$. The challenge arises from the matrix size. If N represents the size of the truncated Hilbert space of the harmonic oscillator that we consider in our calculation, $2N \times 2N$ is the size of the reduced density matrix σ and $2N^2 \times 2N^2$ the corresponding size of the Liouvillean matrix (remember we neglect electrical coherences).

The description of the SD dynamics requires (especially in the shuttling regime) amplitude oscillations of the vibrating dot between 5 and 10 times larger than the zero point fluctuations. For this reason, we are left to study the null space of matrices of typical size of $2 \cdot 10^4 \times 2 \cdot 10^4$. We solved this numerical problem using the iterative Arnoldi scheme.

3.2 The Arnoldi scheme

The Arnoldi scheme is an efficient numerical method for the calculation of the null space, since (i) it allows to work with operators on the system Hilbert space only, and (ii) it requires to look for the best approximation to the null vector in spaces which are typically much smaller that the Liouville space.

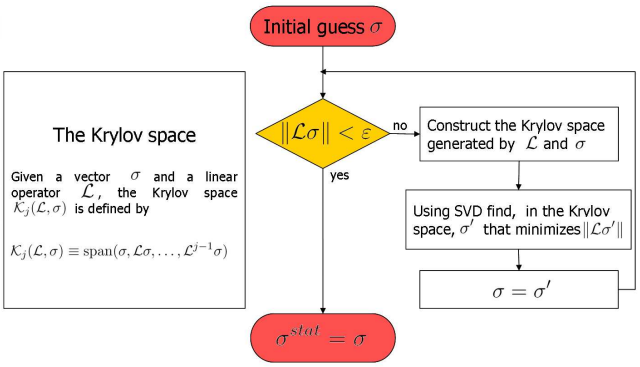

Fig. 2. *Schematic representation of the iterative Arnoldi scheme.*

The central rôle in the Arnoldi scheme is played by Krylov spaces. For a given Liouvillean $\mathcal{L}$ and a temptative matrix σ of the Liouville space we define the Krylov space as:

$$\mathcal{K}_j(\mathcal{L},\sigma) \equiv \text{span}(\sigma, \mathcal{L}\sigma, \ldots, \mathcal{L}^{j-1}\sigma) \tag{8}$$

where j is a small natural number. It is important to note that for the construction of the Krylov space all what we need are the matrices σ, $\mathcal{L}\sigma$, $\mathcal{L}^2\sigma$, ... and not explicitly the superoperator $\mathcal{L}$. The method proceeds by looking for the best approximation of the null vector for the matrix representation of the Liouvillian within the Krylov space $\mathcal{K}_j(\mathcal{L},\sigma)$. We call this vector σ'. This minimization is operated into a space of

size $j+1$, is much less demanding than the one required in the original problem and is performed using singular value decomposition (SVD) [5]. If the criterion $\|\mathcal{L}\sigma' < \epsilon$ for a given threshold value ϵ is not satisfied, we restart the procedure with the improved guess $\sigma = \sigma'$, otherwise we accept the solution. A schematic representation of the Arnoldi iterative method is presented in Fig. 2.

3.3 Preconditioning

The Arnoldi scheme is iterative and can suffer from convergence problems. It is not a priori clear how many iterations one needs to converge and fulfill the convergence criterion. A possible answer to a non-convergent code is, though, to reformulate the problem into an equivalent and (hopefully) convergent form. The basic idea is to find a regular operator $\mathcal{M}$ on the Liouville space, invertible, easy to implement, such that the original problem $\mathcal{L}[\sigma^{\rm stat}] = 0$ can be recast into the form:

$$\mathcal{M}[\mathcal{L}[\sigma^{\rm stat}]] = 0 \tag{9}$$

and that the finite version of the operator $\mathcal{ML}$ gives rise to a (fast) convergent iteration scheme. The operator $\mathcal{M}$ is also known as the *preconditioner*.

The Arnoldi scheme is particularly efficient in finding the best approximation of the eigenvalues and corresponding eigenvectors for those eigenvalues that are separated from the rest of the spectrum. Since we want to calculate the null vector it is important that the preconditioner moves the non-vanishing part of the spectrum far from the origin. For the problem (7) of the stationary solution of our GME, a good preconditioner is represented by the operator $\mathcal{M} = \mathcal{L}_{\rm Sylv}^{-1}$ where

$$\mathcal{L}_{\rm Sylv} = \mathbf{A}\sigma + \sigma\mathbf{A}^\dagger = \begin{bmatrix} A_{00}\sigma_{00} + \sigma_{00}A_{00}^\dagger & 0 \\ 0 & A_{11}\sigma_{11} + \sigma_{11}A_{11}^\dagger \end{bmatrix} \tag{10}$$

and

$$\begin{aligned} A_{00} &= -\frac{i}{\hbar}H_{\rm osc} - \frac{\Gamma_L}{2}e^{-\frac{2x}{\lambda}} - \frac{i\gamma}{2\hbar}xp - \frac{\gamma m\omega}{\hbar}\left(n_B + \frac{1}{2}\right)x^2 \\ A_{11} &= -\frac{i}{\hbar}(H_{\rm osc} - e\mathcal{E}x) - \frac{\Gamma_R}{2}e^{\frac{2x}{\lambda}} - \frac{i\gamma}{2\hbar}xp - \frac{\gamma m\omega}{\hbar}\left(n_B + \frac{1}{2}\right)x^2 \end{aligned} \tag{11}$$

where n_B is the average occupation number of the energy states of the harmonic oscillator in equilibrium with the bath.

4 The three regimes

Once the static density matrix is found, the current is readily calculable from

$$\begin{aligned} I^{\rm stat} &= e{\rm Tr}_{\rm osc}\{\Gamma_R e^{2x/\lambda}\sigma_{11}^{\rm stat}\} \\ &= e{\rm Tr}_{\rm osc}\{\Gamma_L e^{-2x/\lambda}\sigma_{00}^{\rm stat}\}. \end{aligned} \tag{12}$$

Also the noise [2], and even the higher cumulants [4], can be calculated with similar methods. In particular, we find that the Fano factor $F = S(0)/2eI$ (here $S(0)$ is the zero-frequency component of the noise spectrum) can be expressed as

$$F = 1 - \frac{2e\Gamma_R}{I}\mathrm{Tr}_{\mathrm{osc}}\left\{e^{\frac{2x}{\lambda}}\left[\mathcal{Q}\mathcal{L}^{-1}\mathcal{Q}\times\left(\Gamma_R e^{\frac{x}{\lambda}}\rho_{11}^{\mathrm{stat}}e^{\frac{x}{\lambda}}0\right)\right]_{11}\right\}\ . \tag{13}$$

Here $\mathcal{Q}$ is a projection operator that projects away from the stationary state. Very importantly, the pseudoinverse $\mathcal{R}$ of the Liouvillean, defined as $\mathcal{Q}\mathcal{L}^{-1}\mathcal{Q} \equiv \mathcal{R}$ is tractable by similar numerical methods as used in the evaluation of the current (we use the generalized minimum residual method (GMRes)). Before showing results for the current and noise, we discuss an important visualization tool.

We have found that Wigner functions are an excellent investigation tool for the numerical results obtained for the stationary density matrix. The intuitive picture comes from the well-known results in the classical limit: the Wigner representation (or, equivalently, the phase-space representation) of a regularly moving harmonic oscillator is a circle. On the other hand, irregular motion under the influence of external noise gives rise to a Gaussian probability distribution centered at the origin. Since the QD can be either empty or occupied, it is advantageous to introduce *charge resolved* Wigner functions ($n = 0$ corresponds to an empty dot, while $n = 1$ represents the occupied dot), defined as

$$W_{nn}^{\mathrm{stat}}(q,p) = \int_{-\infty}^{\infty}\frac{d\xi}{2\pi\hbar}\left\langle q - \frac{\xi}{2}\right|\sigma_{nn}^{\mathrm{stat}}\left|q + \frac{\xi}{2}\right\rangle \exp\left(i\frac{p\xi}{\hbar}\right). \tag{14}$$

The behavior of the total Wigner distribution as a function of the mechanical damping shows precisely a smooth transition between the dot and the circular structure at high and low damping respectively. The threshold for this transition is given by the effective tunnelling rates of the electrons.

The following picture arises: every time an electron jumps on the movable grain the latter is subject to the electrostatic force $e\mathcal{E}$ that accelerates it towards the right. Energy is pumped into the mechanical system and the dot starts to oscillate. If the damping is high compared to the tunnelling rates the oscillator dissipates this energy into the environment before the next tunnelling event: on average the dot remains in its ground state. On the contrary for very small damping the relaxation time of the oscillator is long and multiple "forcing events" happen before the relaxation takes place. This continuously drives the oscillator far from equilibrium and a stationary state is reached only when the energy pumped per cycle into the system is dissipated during the same cycle in the environment.

It is not difficult to realize that, like for a macroscopic swing, in order to sustain the motion one needs coordination between forcing (here related to the electrical dynamics) and oscillations. This coordination is revealed by the charge resolved Wigner distributions W_{00} and W_{11}. The ring that appears in the total distribution is asymmetrically shared by the empty and charged-dot distributions (Fig. 3).

We study also the current as a function of the mechanical damping (left panel of Fig. 4). At low damping the current saturates, at the "magic" value $I \approx 0.16\omega$ (the frequency of the harmonic oscillator $\omega/2\pi$). This value is independent of the others parameters of the model. Increasing the damping the stationary current drops, more or less rapidly, to a plateau, dependent this time on both the bare tunnelling rate and length. Further increase of the damping does not change the scenario.

If we compare the current results with the Wigner function distribution we can recognize a correspondence between the shuttling charge-position (momentum) correlation and the saturation point, as well as a progressive disappearing of the ring structure in correspondence with the current transition. The high damping plateau in the current sets in when the mechanical oscillator lays into its ground state and

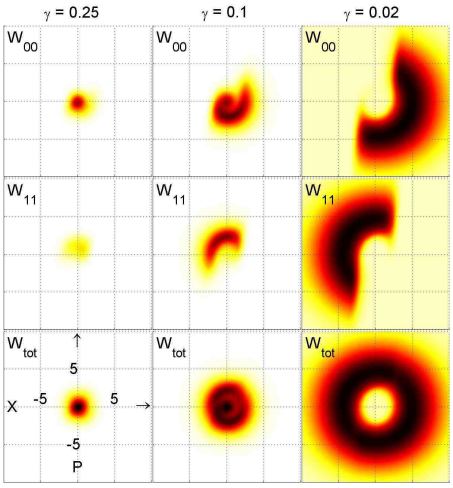

Fig. 3. *Phase space picture of the tunnelling-to-shuttling transition. The respective rows show the Wigner distribution functions for the discharged (W_{00}), charged (W_{11}), and both ($W_{\rm tot}$) states of the oscillator in the phase space. ($\Gamma = 0.05, \lambda = 1$)*

the Wigner distribution function is reduced to a fuzzy spot close to the origin of the phase space.

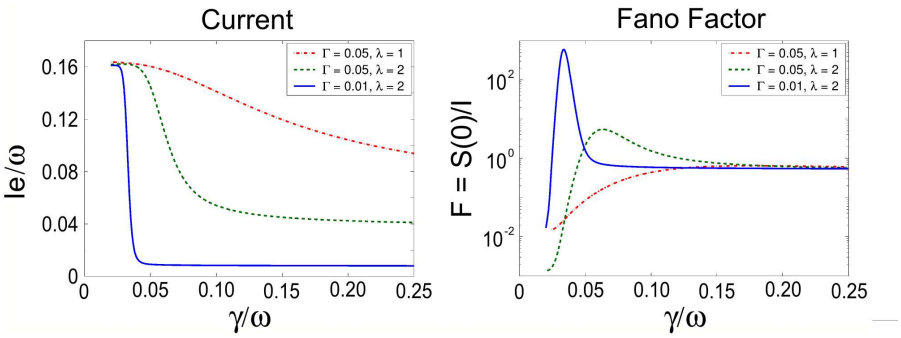

Fig. 4. *Particle stationary current (left) and Fano function (right) of the SD plotted as a function of the damping rate.*

In the right panel of Fig. 4 we present the Fano factor as a function of the mechanical damping γ for different values of the bare injection rate Γ and tunneling length λ. We recognize common features in the three curves. At high damping the Fano factor is of order 1 and (at least for the "most classical" set of parameters

$\lambda = 2x_0$ and $\Gamma = 0.05\omega, 0.01\omega$) close to what we expect from a resonant tunneling system. The discrepancies from the symmetric double barrier are due to the quantum fuzziness in the position of the dot that influences the injection and ejection rates and to the charge dependent equilibrium position of the dot. Diminishing the damping the Fano factors encounter a more or less pronounced maximum and drop finally to very low values for small damping. The maximum at intermediate damping rates is more pronounced and sharper the more classical are the parameters and can reach values of $F \approx 600$ for the most classical case.

A comparison with the current curves (Fig. 4) shows that the peak in the Fano factor corresponds to the transition region from the tunneling to the shuttling current. Similarly the correspondence can be established also with the Wigner function distribution: the region of damping in which tunneling (dot in W_{tot}) and shuttling (ring in W_{tot}) features coexist is associated with a super-poissonian Fano factor. The very low ($F \approx 0.01$) Fano factors for low damping are a signature of the deterministic transport that takes place in the shuttling regime. It is interesting to note that this regularity persists also deep in the quantum regime as can be seen for $\Gamma = 0.05$ and $\lambda = 1$. The relative uncertainty in the amplitude of the oscillation (see Fig. 3) does not seem to influence the current noise.

5 Conclusions

In conclusion, we have presented a numerical technique for solving the generalized Master equation governing an archetypal model of shuttle device. The obtained numerical results are interpreted with the help of phase space representations and allow to identify three operating regime of the SD. We believe that the methods discussed here are also applicable to many other quantum transport situations, where the matrix representations of the relevant operators are very large, but where only certain extremal eigenvalues are important.

References

1. T. Novotný, A. Donarini, and A.-P. Jauho, Quantum Shuttle in Phase Space, Phys. Rev. Lett. **90**(25), 256801 (June 2003).
2. T. Novotný, A. Donarini, C. Flindt, and A.-P. Jauho, Shot Noise of a Quantum Shuttle, Phys. Rev. Lett. **92**(24), 248302 (June 2004).
3. C. Flindt, T. Novotný, and A.-P. Jauho, Current noise in a vibrating quantum dot array, Phys. Rev. B **70**, 205334 (November 2004).
4. C. Flindt, T. Novotný, and A.-P. Jauho, Full counting statistics of nano-electromechanical systems, Europhys. Lett. **69**(3), 475 (December 2004).
5. T. Eirola and O. Nevanlinna, Numerical linear algebra; iterative methods, Lecture notes, Helsinki University of Technology, 2003.